1. INTRODUCTION

Breast cancer is one of the most common tumours and one of the leading causes of death in women [1]. According to estimates of lifetime risk by the U.S. National Cancer Institute [2], in the U.S about 13% of women, which means 1 in 8 women, will develop breast cancer in their lifetime. Many countries (*e.g.* UK, Italy, Australia) offer screening programs to women for prevention, typically between 50 and 70 years of age, since early diagnosis and therapy can have huge impact in terms of death rate and quality of life [3].

Breast screening essentially relies on X-ray mammography, which is the first line of defence in the early diagnosis of the breast cancer. However, mammography is less accurate in patients with dense glandular breasts [4], including young women, with reported sensitivity as low as 48% [5].

Magnetic resonance imaging (MRI) is the most sensitive technique to diagnose invasive breast cancer, with good performance even in dense breast tissue, but because of the increased sensitivity it can also lead to false positive results [6]. Moreover, MRI is characterized by high costs and long examination times, which prevent its routine use for screening purposes.

Another important technique, non-invasive and with an excellent spatial resolution which is used in the clinical practice, is breast ultrasonography (US). It is often applied as complementary breast imaging technique in women with mammographically dense breast tissue, permitting detection of small occult breast cancers [7]. The technique is not particularly expensive, but US data interpretation is strongly operator's dependent [8].

Positron Emission Tomography (PET) is also applied to breast imaging. It is important in order to obtain information on the nature of the detected lesion. PET is also effectively applied in cancer staging. However, it is an expensive technique and involves the administration of a radioactive tracer [9].

It is worth mentioning that breast imaging aims not only at diagnosing diseases, but also at monitoring therapy. For the latter use MRI is typically applied, but mammography is still the gold standard among imaging techniques that aim at diagnosing breast pathologies. Therapy monitoring involves several imaging sessions concentrated in a short time period. Since the use of ionizing radiation can have adverse effects that should be avoided, it is evident that new breast imaging methods are needed.

Optical mammography is an emerging diagnostic tool which can provide information on breast tissue composition and related physiological or pathological parameters as well as tissue structure. The technique is absolutely non-invasive thanks to the use of visible and near-infrared (NIR) light, which is a non-ionizing radiation, able to cross some centimetres of biological tissue, offering a real opportunity to investigate the whole breast volume *in vivo*. Moreover, other advantages of optical mammography are its relative low instrumentation costs and capability to investigate dense breasts, typical of young women, covering X-ray mammography limits. Indeed, optical mammography could be effectively applied as a complementary diagnostic technique. Further, optical mammography can be performed at multiple wavelengths so as to combine imaging and spectroscopic information for lesion detection and characterization at the same time.

Besides to all these advantages, optical mammography has also some limits. The technique is able to provide breast images with low spatial resolution, leading difficult the detection of tumours smaller than 1 cm. This is an intrinsic limit of the technique, depending on NIR light diffusion in biological tissue. To overcome this problem, multimodality imaging approaches are being developed, in which optical mammography is combined with the conventional ones (X-ray, MRI, US and PET) [10-13] providing complementary information. Another limit affecting optical mammography is linked to the signal acquired in breasts of big size: it has often low information content, resulting useless for diagnostic purposes. This is a contingent limit which could be overcome by the technological advances.

The physical basis of optical mammography, operating in the visible and near infrared light spectrum (600-1100 nm), is the difference in propagation of light through healthy tissue and tumours. Light is attenuated by two main phenomena: absorption, which destroys the incoming photons, reducing the intensity of the transmitted light, and scattering, which changes the direction of propagating photons. Light absorption is caused by chromophores, such as haemoglobin, water, lipid and collagen, which are present in the breast tissue; light scattering originates, instead, from changes of the refractive index occurring between connective tissues and cell constituents. Both absorption and scattering phenomena are strongly wavelength-dependent: at short visible wavelengths, they occur with comparable probability, while at longer wavelengths (red and NIR), the scattering events become dominant, but both processes are much less probable, allowing a significantly increased light penetration. As a consequence, to get access to deeper tissue structures for diagnostic purposes, wavelengths in the range between 600 and 1100 nm, named 'therapeutic window', are usually chosen.

Light transport through highly scattering media can in principle be described using the electromagnetic theory directly based on Maxwell's equations and taking into account the wave nature of light. However, due to the complex structure of tissue, the application of the electromagnetic theory is extremely difficult and not of practical use. Alternatively, the radiative transport theory can be considered. Relying on the particle nature of light, it describes the photon transport in tissue as the propagation of a particle flow. Further approximations of the transport theory lead to the 'Diffusion theory', which is mathematically less rigorous than the electromagnetic theory, yet providing an analytical solution of the problem. The scattering events are supposed to be isotropic and strongly dominant over the absorption events, and several scattering events need to occur into the medium before the description provided becomes accurate enough. Actually, exact solutions of the radiative transport equation have recently been introduced for specific geometries [14] and other theoretical models are available [15]. However, the diffusion approximation is still the most widely used theoretical approach in the biomedical field, because it provides a simple analytical solution to the problem of photon propagation in highly scattering media, such as biological tissues [16].

Different substances typically absorb at different wavelengths, so the measurement of the absorption spectrum of a medium allows in principle for the identification of its constituents. Then, to obtain information on tissue composition, measurements must be performed at several wavelengths. In fact, the absorption coefficient μ_a of tissue at any wavelength λ is due to the superposition of the contributions from the different constituents, given by the product of the intrinsic absorption ε, known in literature, and the concentration C of each constituent, as in the following formula (Beer's Law):

$$\mu_a(\lambda) = \sum_{i=1}^{n} \varepsilon_i(\lambda) C_i \quad (1.1)$$

Concerning breast tissue, there are five main constituents to consider (oxy- and deoxygenated haemoglobin, water, lipid and collagen, see Figure 1), so to estimate their concentration, measurements at a minimum of five wavelengths have to be performed.

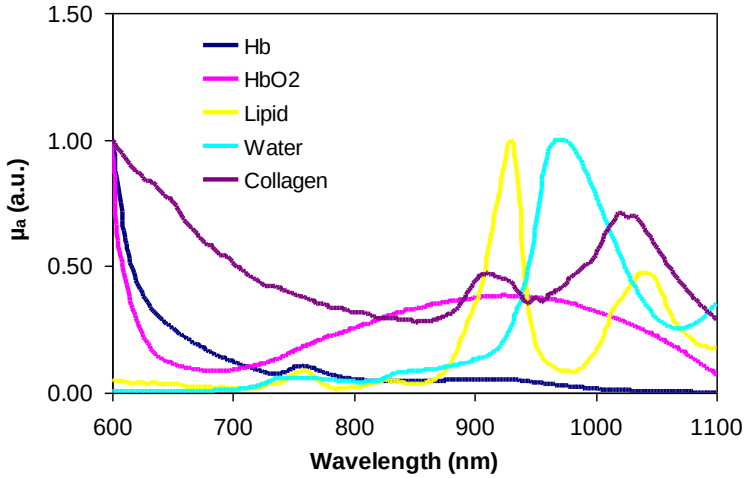

Figure 1: Normalized extinction spectra of the main constituents of the breast tissue.

As shown in Figure 1, blood strongly absorbs in the red spectral range, while lipids, water and collagen are characterized by maximum absorption at wavelengths longer than 900 nm. The need to operate at several wavelengths led to a careful choice of their value, which had to take into account also their commercial availability. Generally, the choice fell on red wavelengths (*e.g.* 635-685 nm) because they are most sensitive to the blood components, in particular to the deoxy-haemoglobin. Higher wavelengths below 800 nm are usually used for the oxy-haemoglobin. The wavelengths in the near-infrared range, up to 900 nm are used for the other two important components of biological tissues, such as lipids and water. In particular the wavelengths around 930 and 1040 nm, where dominant peaks are present, are used for lipids; the wavelengths around 975 nm are used for the discrimination of water, because here it reaches a higher absorption value than the other chromophores. If, on one hand, the blood investigation is useful for the breast cancer detection due to its higher vascularization than healthy tissue, another important component to be investigated for diagnostic purposes is the collagen, whose absorption is dominant around 1100 nm. In fact, it is one of the main components of soft and hard tissues, and in particular of the breast one. Its contribution to tissue absorption has to be considered for a correct quantification of the tissue composition. Furthermore, collagen seems to be involved in the development of breast cancer and thus sensitivity to collagen could be relevant for cancer detection.

As mentioned above, scattering is the other light attenuation phenomenon due to the presence at microscopic level of refractive index discontinuities in biological tissues. In particular both the size and density of scattering centres affect the scattering properties, so their assessment can provide information on the structure of tissues. The reduced scattering coefficient μ'_s decreases monotonically upon increasing wavelength, without characteristic peaks. It is related to the scattering amplitude *a*, which provides information on the density of scattering centres, and to the scattering power *b*, which gives information on their size, according to the Mie theory:

$$\mu'_s(\lambda) = a(\lambda)^{-b} \quad (1.2)$$

High values of *a* correspond to denser tissues, whereas smaller scattering centres, so high values of *b*, lead to steeper slope. An example of reduced scattering spectra related to two different breast patterns is reported in Figure 2. The steepest spectrum (blue) refers to fibrous breast which is characterized by smaller scattering centres with respect to the adipose breast, which has instead a flat spectrum (pink).

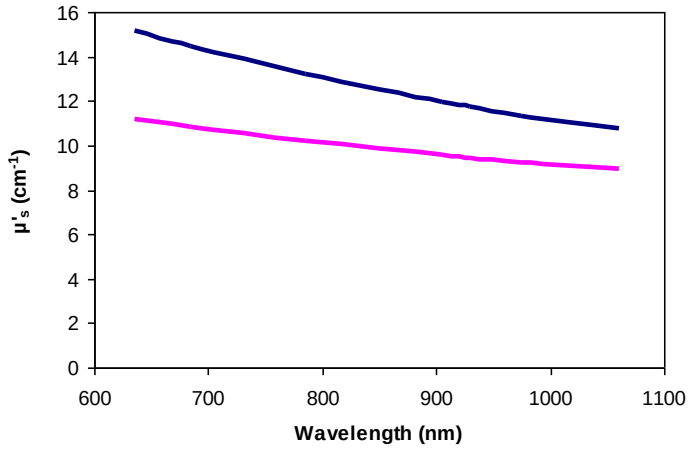

Figure 2: Reduced scattering spectra of two different breast patterns. Blue line refers to fibrous breast and pink line to adipose one.

Since both absorption and scattering contribute to light attenuation and have independent origins, it is important to use a technique capable to discriminate between these two optical phenomena.

A number of different implementations to optical mammography have been evaluated. The first procedure of transillumination of breast was the **diaphanography**, where light from a lamp was diffused throughout the tissue and randomly scattered [17]. Opaque lesions formed shadows on the surface of the breast which acted as a screen. The problem was that the deeper the lesion, the greater the distance from the 'screen', and the less the contrast. It had sensitivity only at the detector side. Improved contrast and resolution was achieved by employing a narrow-beam light source and by scanning it in tandem with a localized optical detector. This approach enhances detectability of deep optical inhomogeneities and provides high sensitivity to superficial structures near both the source and the detector side. More recently, the approach based on the use of steady state light sources (*i.e.* **continuous wave**) and detectors allowed for dynamic measurements and spectral information over a broad continuous spectrum. A drawback is its inability to discriminate between absorption and scattering properties unless a complex tomographic scheme is adopted.

To overcome these limitations, richer information content can be achieved by performing spectroscopy or imaging in either the frequency domain, where the light source intensity is sinusoidal modulated, or in the time domain, where the light source is pulsed. These two implementations differ in the instrumentation used.

The **frequency domain** approach is based on modulating the intensity of the light source at a certain frequency (usually of the order of 100 MHz) and detecting the changes in amplitude and phase of the optical signal emerging from the tissue. These parameters can provide information to characterize both absorption and scattering properties of the tissue. Accurate estimates of the absorption and scattering properties generally require measurements to be performed on a wide range of the modulation frequency.

The **time domain** approach consists of injecting a short light pulse (typically with a duration of the order of 100 ps) into the tissue and measuring the distribution of the photon time-of-flight emerging from at a certain distance from the injection point. Scattering and absorption events, occurring during light propagation through the tissue, cause attenuation, delay and broadening of the injected pulse. The scattering essentially delays the collected pulse, as each scattering event changes the direction of photon propagation and, thus, photons move along trajectories that are much longer than the distance between the injection and the detection points: the higher the scattering, the longer the delay. The absorption influences the steepness of the temporal tail of the detected photon time-

of-flight. The effects of absorption can be mostly seen at long times, that is on the pulse tail, because the longer the photons stay in the medium, the higher the probability of an absorption event. Thus, strong absorption means that many photons are removed from the temporal tail of the pulse and its slope becomes steeper.

The aim of this chapter is to provide an overview on the applications of time-domain diffuse optics to the assessment of breast physiology and pathology. As we will see different applications were proposed, ranging from breast lesions detection and characterization, using endogenous (§ 2) or exogenous (§ 3) contrast, to monitoring neoadjuvant chemotheraphy (§ 4) and to the assessment of breast density as strong cancer risk factor (§ 5). As mentioned, the time-domain approach permits to uncouple absorption from scattering contributions and to derive tissue optical properties *in vivo*. Furthermore, Time-Correlated Single-Photon Counting (TCSPC) is the measurement technique often chosen to acquire time-resolved fast and weak optical signals: it is well suited for biological tissue spectroscopy because the overall attenuation of biological tissues is in the order of 8-10 OD and the temporal dynamics of photon migration in diffusive media last for 1-5 ns. [17].

2. TIME-RESOLVED OPTICAL MAMMOGRAPHY WITH ENDOGENOUS CONTRAST

Diffuse optical imaging techniques use measurements of transmitted light to produce spatially resolved images. Images of the absorption or scattering properties of the tissue, or other physiological parameters (such as haemoglobin, lipid, water, collagen) may be generated. As reported in the introduction, a wide spectral range in the NIR region is necessary in order to get information on the main constituents of the breast tissue.
Over the past, the use of wavelengths longer than 850 nm was often prevented by limitations on available commercial detectors, in fact most initial breast imaging studies were performed at 2-4 wavelengths within the range of 650-850 nm. More recently, longer wavelengths have became available, allowing operating over an extended spectral range.

An example of set-up of a time domain scanning optical mammographs, working at 7 wavelengths in the extended spectral range 635-1060 nm, is reported in Figure 3.

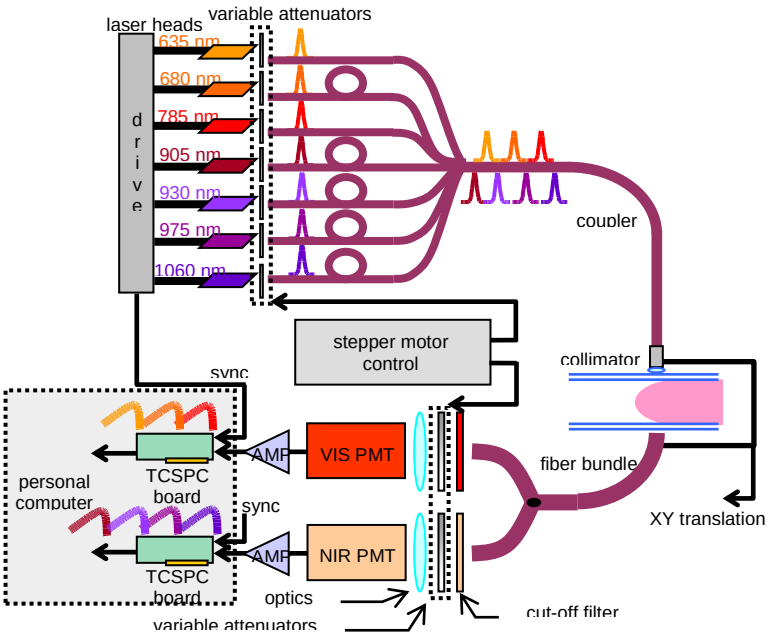

Figure 3: Instrument set-up. NIR, near-infrared; PMT, photomultiplier tube; TCSPC, time-correlated single photon counting.

The set-up was developed by the research group at Politecnico di Milano, Italy, and it is currently applied in a clinical trial [19]. Briefly, seven pulsed diode lasers (PDL Heads, PicoQuant, Germany) are presently used as light sources emitting at 635, 680, and 785 nm (VIS), and at 905, 930, 975 and 1060 nm (NIR), with average output power of ~1-4 mW, temporal width of ~150-400 ps (full width at half maximum, FWHM), and repetition rate of 20 MHz. A photomultiplier tube (PMT) for the detection of VIS wavelengths (sensitive up to 850 nm, R5900U-01-L16, Hamamatsu, Japan) and a PMT for NIR wavelengths (sensitive up to 1100 nm, H7422P-60, Hamamatsu, Japan) are used for the detection of the transmitted light. Two PC boards for time-correlated single-photon counting (SPC134, Becker&Hickl, Germany) allow the acquisition of time-resolved transmittance curves at VIS and NIR wavelengths, respectively. More details on the instrument are reported in [20].

Important results on the potential of time-resolved transmittance imaging for optical mammography were obtained within the European project 'Optimamm: Imaging and characterization of breast lesions by pulsed near-infrared laser light', performed in 2000–2004. In particular, within this project, extensive clinical data were collected by partners in Germany [21] and Italy [22]. Time domain scanning optical mammographs operating in transmittance geometry on the compressed breast were developed and tested by both research groups. Images were acquired from both breasts in two views (cranio-caudal and medio-lateral, or cranio-caudal and oblique), in agreement with routine clinical practice for X-ray mammography for easier comparison between optical images and standard X-ray mammograms for the retrospective assessment of the optical technique.

In this work, the attention is focused on the results of the most extensive clinical trials performed in Berlin and Milan. In particular, the group in Berlin [21] developed a triple wavelength (670 nm, 785 nm, 843/884 nm) instrument and applied it on 154 patients, suspected of having breast cancer. Off-axis mammograms, with 2 cm offset between the transmitting and detecting fibre bundle, were also recorded upgrading the instrument. Off-axis scans were limited to a region of interest, presumably containing a tumour, to reduce the overall recording time. This approach was performed in order to infer the location of the tumour along the compression direction. Time-window analysis of distributions of times of flight of photons recorded at a large number of scan positions was used to obtain the optical mammograms. Additionally, absorption and reduced scattering coefficients were used to generate mammograms. These coefficients were derived by the time-resolved transmittance curves measured at each scan position and calculated within the diffusion approximation for a homogeneous tissue slab. They were then used to derive information on the constituent concentration. Setting the percentage content of water and lipids to fixed values, total haemoglobin concentration and blood oxygen saturation were estimated from 2 or 3-wavelength data. Seventy-two out of 102 histological confirmed tumours (71%) were detected retrospectively in both optical projection mammograms, and 20 more lesions (20%) were detected in one projection only.

The group in Milan [22] initially developed an instrument operating at 4 wavelengths (683, 785, 913 and 975 nm). In particular, 2 wavelengths were longer than 900 nm (*i.e.* 915 and 975/985 nm) to increase the sensitivity to lipids and water, which show major absorption peaks in that wavelength range (Figure 1). To investigate the diagnostic potential of shorter wavelengths, the instrument was modified adding other wavelengths shorter than 700 nm (637 and 656 nm). The several upgrades of the instrument led to collect mammograms at a different number of wavelengths, from 4 to 7, even if the final version operated at four wavelengths (637, 785, 905 and 975 nm).
The instrument, in the several configurations, was tested on a total of 194 patients with 225 malignant and benign lesions. Forty-one out of 52 cancers (79%) were detected in both views and 9 more (17%) in just one view. Concerning benign lesions, a significant number of cysts was

analysed (n = 82), achieving a detection rate of 83% in both views, which came to 90% if detection in a single view was accepted.
A synthetic scheme of the main information of the two clinical trial is reported in Table 1.

Table 1: General information of the 2 main clinical trials within the European project Optimamm

Group	N° patients	N° wavelengths	Spectral range	N° lesions	Detected lesions in 2 views	Detected lesions in 1 view
PTB	154	3	670-884 nm	102*	72	20
Polimi	194	4	637-985 nm	225	130	21

* only lesions validated by histology

Images at all wavelengths were constructed by plotting the number of photons collected within a selected time window as well as the reduced scattering coefficient. Also in this case, data analysis was performed using the time gated approach. As first step, a reference position was selected far from boundaries and possible inhomogeneities. This was performed to avoid the dependence of gated intensity images on the temporal position and width of single transmittance curves. The time distribution of data acquired in that position was divided into 10 time windows, each one collecting 1/10 of the total number of counts. The same time gates were then used in any other position of the scanned area to build gated intensity images. The 8^{th} gate, on the tail of the pulse, was routinely applied for breast imaging. The estimated absorption and reduced scattering coefficients (μ_a and μ'_s, respectively) were average values along the line of sight, as obtained from the best fit of the experimental data with the analytical solution of the diffusion equation, with extrapolated boundary condition, for a homogeneous slab [23, 24].
For each breast projection and wavelength, the estimate of bulk optical properties was limited to a reference area excluding the boundaries and marked inhomogeneities, but still including most of the breast. To select that area, the time-of-flight (*i.e.* the first moment of the time-resolved transmittance curve) was calculated for each image pixel, and only pixels with time-of-flight greater than or equal to the median of the distribution were included in the reference area. The absorption and reduced scattering values of bulk tissue were then obtained by averaging the absorption and reduced scattering coefficients over the reference area.

An example of gated intensity images acquired at six wavelengths from a patient with a lobular invasive carcinoma in her left breast is reported in Figure 4. The tumour is visible at all wavelengths between 637 and 785 nm, but the contrast reduces upon increasing wavelength [25]. Adipose or fibrous structure can be easily observed at longer wavelengths, 916 and 975 nm respectively. For example, the mammary gland, together with water-rich structures such as liquid cysts, can generally be identified at 975 nm. In the case of the adipose breast reported in Figure 4, a stronger absorption at 975 nm is observed in the lower and anterior part of the breast. A same high absorption area is more evident in the denser breast reported in Figure 5(top). In fact, the mammary gland, which is detected as an opaque area in the x-ray mammogram, is well observed as a strongly absorbing region of similar shape in the gated intensity image at 975 nm. In that image, the mammary gland overlaps a cyst, masking the contribution of the lesion to the overall light attenuation. However, the presence of the cyst is revealed by the weak absorption at 905 nm, in agreement with a lower lipid content than in the surrounding tissue. Moreover, cyst with a liquid nature, are usually characterized by low scattering. In fact, it is evident from all scattering images reported in Figure 5(bottom).
Figure 6 reports images from a patient with a fibroadenoma in her right breast. The detection of fibroadenomas often proved to be problematic. When identified, they are generally characterized by higher absorption at 975 nm and sometimes even in the red (637–683 nm), as observed in Figure 6. The marked absorption at 975 nm is likely related to the high water content, but it might also be at least in part due to collagen, with absorption increasing both at short (<700 nm) and long (>900 nm) wavelengths [26]. From Figure 6, we can see how absorption at 975 nm follows, even though with

clearly lower spatial resolution, the patterns identified in the x-ray mammography, with a region of strong absorption starting at the fibroadenoma location and a second area of marked absorption in retroareolar position. In contrast, data acquired on the lipid peak (905–916 nm) typically show opposite behaviour, adipose tissue being transparent to x-rays. However, in the latter case the correspondence is often not complete, possibly due to some contribution from haemoglobin around 900 nm. In Figure 6, dominant absorption is observed in median position, both at 683 and 975 nm. The area corresponds to an x-ray dense region, and is possibly highly vascularized fibro-glandular tissue.

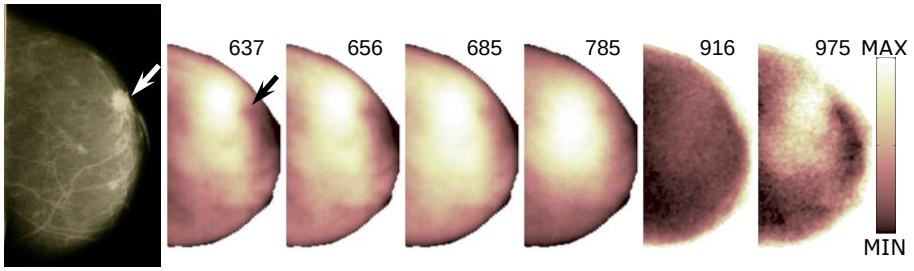

Figure 4: X-ray mammogram and late gated intensity images (637, 656, 685, 785, 916, and 975 nm) of the left breast (cranio-caudal view) of patient #146, bearing a lobular invasive carcinoma (max. diameter = 15 mm).

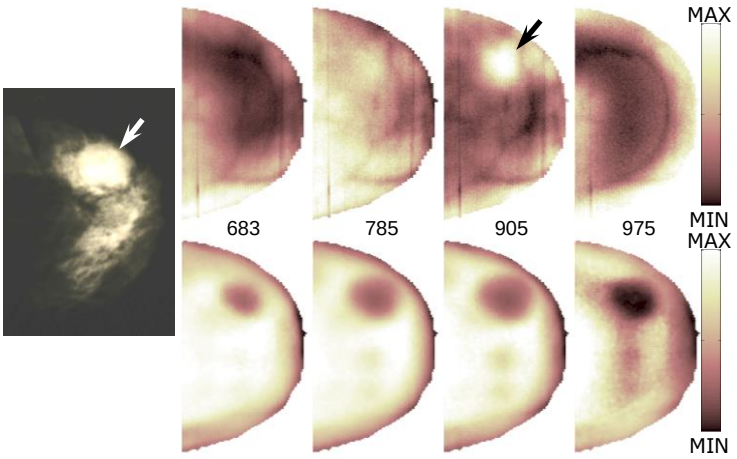

Figure 5: X-ray mammogram, (top) late gated intensity and (bottom) scattering images (683, 785, 905, and 975 nm) of the left breast (cranio-caudal view) of patient #185, bearing multiple cysts (max. diameter of the cyst indicated by the arrow = 38 mm).

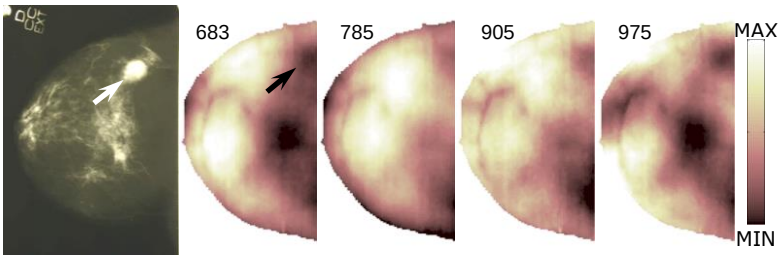

Figure 6: X-ray mammogram and late gated intensity images (683, 785, 905, and 975 nm) of the right breast (cranio-caudal view) of patient #180, bearing a fibroadenoma (max. diameter = 20 mm).

In conclusion, both studies had similar detection rates for malignant breast lesions. On average, late gated intensity images at short wavelengths (*i.e.* < 700 nm) provided the highest tumour-to-healthy contrast and also the highest contrast-to-noise ratio. At short wavelengths, blood absorption is dominant, so the contrast was attributed to high blood volume in the lesion. For the estimate of tissue composition and specifically to quantify constituents in the detected lesions, simple perturbative approaches were used, considering a single spherical lesion in an otherwise homogeneous background [27, 28]. Both studies confirmed significantly higher haemoglobin

content in the lesion, as compared to the surrounding healthy tissue, while blood oxygen saturation proved to be a poor discriminator.

In parallel, within the same project, also the potential of time-resolved optical tomography of the uncompressed breast as a diagnostic tool was tested [29]. This limited study was performed on 24 subjects, including 19 cases with a specific lesion. In this approach, the patient lies prone with her breast pendent through a hole, while sources and detectors (16 in total) are distributed along one or more rings around the breast. For each source, the time-of-flight distributions of the photons were recorded by all detectors simultaneously. The system operated at 2 wavelengths (780 nm and 815 nm). Thus, for lesion detection and identification they relied on absorption and scattering images. Seventeen out of 19 cases of lesions of different nature were detected by optical images.

In 2005, another time-domain optical mammograph (softscan, Art, Canada) operating at four wavelengths (760, 780, 830, and 850 nm) was developed and applied on 49 women of different age [30]. For all patients absolute bulk and local values of breast constituent concentrations were retrieved. In the 23 cases imaged with suspicious masses, the optical images were consistent with the mammographic findings. Also consistent differences between malign and benign cases were found. In particular, the discrimination based on deoxy-haemoglobin content was statistically significant between malignant and benign cases.

A multi-channel time-resolved optical mammography prototype for breast cancer screening, operating at three wavelengths (765, 800 and 835 nm), was developed by Ueda et al. [31]. A tomographic approach was used to collect data by using a hemispherical cup and a liquid-coupled interface since the breast was uncompressed and a non-contact optical fibre approach was used. Image reconstruction was performed by using the time-resolved photon path distribution (PPD). Early arrival photons were used to improve the spatial resolution. Few cases of tumour detection were evaluated, showing that the lesion could not be detected using the peak photon region, whereas high concentration of haemoglobin could be derived using the early arrival photons.

3. OPTICAL MAMMOGRAPHY WITH EXOGENOUS CONTRAST AGENT

Together with the development of experimental methods for NIR imaging, the use of contrast agents for diffuse optical imaging was considered, aiming at improving the detection of carcinoma. Ideally, the contrast agent should accumulate selectively in the tumour, but not in healthy tissue, in order to increase the contrast between the two areas. Fluorescent contrast agents with excitation and emission in the NIR spectral range are usually considered for optical application, since they allow for deep penetration into breast tissue and are coupled to a limited tissue autofluorescence. Thus, the fluorescence signal coming from the contrast agent localized in the lesion would be dominant with respect to the one coming from the background, leading to an increased contrast.
Nowadays, no contrast agents have these specific features. The only contrast agent that is approved for clinical use and is suitable for breast imaging is Indocyanine Green (ICG). While it is characterized by strong absorption and fluorescence in the NIR wavelength range, it does not provide selectivity for tumour tissue. It operates as blood pool contrast agent: it stays in the vascular system for a long time period and the tumour-healthy contrast is achieved by exploiting its slower kinetics in the tumour, due to an increased resistance of the tumour vasculature to blood flow.
An exploratory study of time domain optical mammography with ICG was performed by the Berlin research group [32]. In particular, for this purpose the previously developed multichannel laser pulse mammograph, (briefly described in § 2), was upgraded for fluorescence measurements both in transmission and reflection [33]. The same planar geometry, with the breast slightly compressed between two parallel glass plates, was used to detect fluorescence of a contrast agent in the breast at high sensitivity. A picture of the final device is reported in Figure 7.

Figure 7: Fluorescent mammograph. Reprinted with permission of …

The instrument was upgraded also in terms of spectral range: a new picosecond diode laser with emission wavelength at 1066 nm was added for a better reconstruction of the constituent concentration, whereas the other 3 wavelengths were modified, emitting in this case at 660, 797 and 934 nm. The most important upgrade was the introduction of the excitation laser emitting at 780 nm for fluorescent images. Details on the instrumentation are reported in [33]. Preliminary measurements were performed administrating the contrast agent intravenously by a bolus followed by an infusion and data were recorded 30 minutes after the end of the infusion of the contrast agent, corresponding to the extravascular phase. Raw absorption and fluorescence mammograms were dominated by the absorption of the excitation and fluorescence radiation by blood. The carcinoma, cannot be detected in the fluorescence mammogram because of cancellation effects. The higher fluorescence intensity of the carcinoma is in fact compensated for by the higher absorption of laser and fluorescence radiation due to its increased blood content. In order to eliminate the inhomogeneous background absorption of the breast tissue and recognize fluorescent objects with a higher contrast, ratio images obtained dividing the normalized total fluorescence counts by the normalized total laser photon counts were calculated.

Preliminary results in which the system was tested on a patient bearing a tumour demonstrated the good sensitivity of the fluorescent optical mammography. The small amount of the extravasated ICG in the extracellular space of the carcinoma, which generates the fluorescent signal, could be detected, allowing one to distinguish between malignant and benign lesions.
Fluorescence ratio mammograms in 68 years old woman with 22 mm invasive ductal carcinoma are reported in Figure 8.

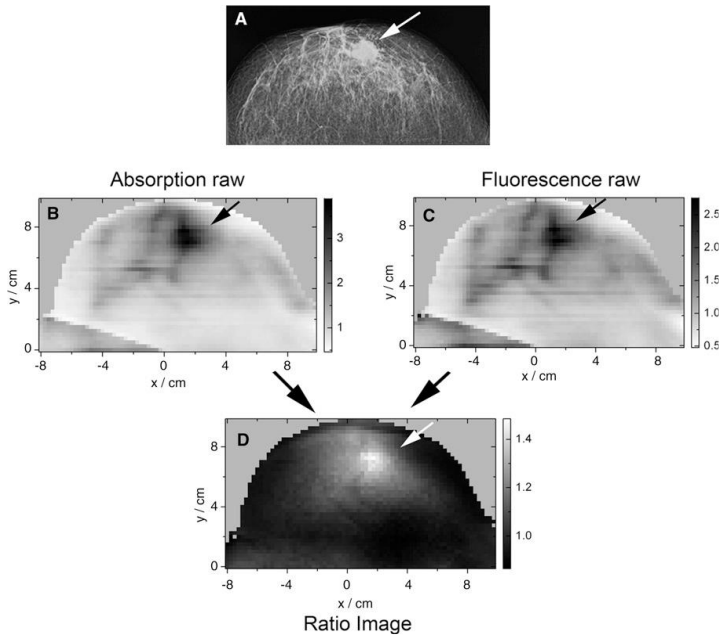

Figure 8: (A) Conventional X-ray mammogram, (B) Absorption and (C) Fluorescence raw mammograms, (D) Ratio mammograms obtained dividing normalized fluorescence image data by normalized absorption image data. Lesion is indicated by the arrow. Reprinted with permission of RSNA from Poellinger et al.[]

Figure 8 shows that in ratio fluorescence image the detection of the tumour is possible with a better contrast. Moreover other structures such as blood vessels that are visible in absorption and fluorescence images are largely eliminated, enabling a clear demarcation of tumour. Of course, a bigger population was needed to test the capability of the fluorescence optical mammograph in discriminating breast tumours.

A further study was then performed by the same research group with a similar instrument set-up [34]. The aim of latter study was to perform fluorescence NIR imaging with early and late enhancement of ICG, corresponding to the vascular and extravascular phases of contrast agent enhancement, respectively, for the detection of breast cancer and the discrimination between benign and malignant breast lesions. Twenty women having 21 suspicious breast lesions were investigated, including 13 malignant and 8 benign lesions. The breast was imaged by on-axis movement of the source and detection fibre bundle at a step size of 2.5 mm, and optical mammograms were recorded in 5–10 minutes. For the measurements, the contrast agent was administered intravenously by a bolus followed by an infusion and data were recorded before, during and after the end of the infusion of the contrast agent. The images acquired before the injection of the contrast agent were used to measure the intrinsic absorption and scattering properties of the breast and the corresponding autofluorescence. To get information on the early and late fluorescence, absorption and fluorescence data were recorded during and after the infusion of ICG, and then the ratio of the images was calculated. For data analysis the total photon counts of the transmittance curve, instead of the photon counts in a selected time window, were used to improve the signal-to-noise ratio.

Only for two lesions (one benign and one malignant) increased autoflorescence was observed with respect to the background tissue, whereas no significant variations were observed in the remaining 19 cases. Malignant lesions were correctly defined in 11 or 12 (depending on the reader) of 13 cases, and benign lesions were correctly defined in 6 or 5 (depending on the reader) of 8 cases with late-fluorescence imaging. Significant differences in the discrimination between malignant and benign lesions were observed using the early-fluorescence ratio mammograms with respect to the late one, indicating that late fluorescence ratio mammograms highlight malignant tumour well with a good contrast against the healthy tissue.

The here presented study on optical mammography with ICG led to good results for what concerns the discrimination between healthy and tumour tissue. Of course, the effectiveness of the system in detecting lesions and the method of imaging reconstruction need to be further tested on a wider population.

4. OPTICAL MAMMOGRAPHY FOR THERAPY MONITORING

Chemotherapy is widely used in the treatment of locally advanced breast cancer before surgery to reduce the tumour size. Monitoring the response to therapy can improve survival and reduce morbidity. Moreover, the immediate knowledge of the individual response to the treatment reduces useless exposure to ineffective drugs with heavy side effects.
Most of the work performed in the field of therapy monitoring concerned chemotherapy was performed using continuous-wave and/or frequency domain set-ups [35, 36].
However, recently time domain optical imaging of the response to hormone therapy has also been developed. In particular, the UCL three-dimensional time-resolved optical imaging system (briefly described in § 2) was used to monitor the response to neoadjuvant chemotherapy in 3 patients bearing advanced breast cancer. The system is characterized by 2 palsed lasers emitting at 780 and 815 nm, which are transmitted to the breast through 31 optical fibers. Details on the instrument set-up can be found in [37]. The patient lies prone with her breast pendant in the liquid-coupled patient interface, as reported in Figure 9.

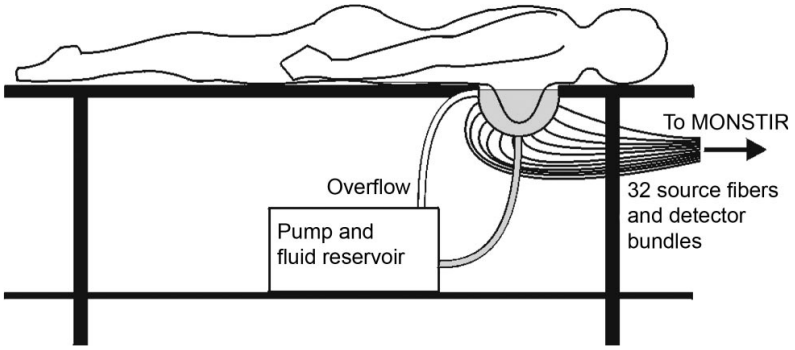

Figure 9: Fluid-coupled patient interface for the 3D optical breast imaging. The patient lies with her breast pedant in a hemispherical cup filled with scattering fluid. Reprinted with permission of OSA from Enfield 2007.

Three optical imaging sessions were performed. The first scan was performed before the start of the treatment; a second scan in the middle of the treatment, and the third one before surgery, when the treatment was completed. Both breasts were scanned, taking 3 minutes for each scan.
Three-dimensional (3D) images were generated from the data using the time-resolved optical absorption and scatter tomography (TOAST) reconstruction package developed at UCL [38].
After the reconstruction of the 3-D images of absorption, scattering and blood parameters, a two-dimensional (2D) coronal slice was extracted from each one in correspondence of the maximum contrast point in the lesion. Then, two circular areas of that image were selected: one containing the tumour and another one related to the background medium (out of the tumour area and the coupling fluid). Similarly, equivalent areas from the contralateral healthy breast were also analysed. In this way, changes in physiological and optical properties within the tumour and in the rest of the breast were evaluated during the course of therapy [39].
All three patients showed changes in both optical and physiological properties in the region of the tumour compared to the rest of the breast. In two patients, a good response to the chemotherapy treatment led to a reduction of the tumour. A decrease of the tumour total haemoglobin was observed in the optical images performed within the treatment. In the third patient a lack of response to therapy was observed and this type of response was also seen in the optical images scan within the treatment.

The present study showed good preliminary results on monitoring tumour response to chemotherapy using time domain optical tomography. Of course, a large number of cases has to be evaluated to establish the capability of the technique and confirm the strong correlation with treatment outcome obtained with very few study cases.

5. OPTICAL MAMMOGRAPHY FOR BREAST DENSITY ASSESSMENT

Breast density is a recognized independent risk factor for developing breast cancer [40,41]. At present, breast density assessment is based on the radiological appearance of breast tissue, requiring the use of ionizing radiation. Its non-invasive estimation would certainly be of diagnostic interest. Optical techniques could contribute to assess breast density in a non-invasive way. A study on the direct correlation of breast density with optically derived main breast constituents (water, lipids, collagen, and haemoglobin) could lead to a better understanding of the role of mammographic density in breast cancer risk assessment. In particular, collagen is an important constituent of breast tissue that seems to be involved in the onset and progression of breast cancer. Furthermore, collagen, as a major constituent of stroma, is expected to be related to breast density [42-44]. Thus, sensitivity to collagen content could be relevant for breast cancer development risk and its quantification by optical means could provide useful diagnostic information.

In this line, an on-going clinical study performed with a 7-wavelength (635-1060 nm) time domain instrument (reported in Figure 3) realized by the research group at Politecnico di Milano has given promising preliminary results [19, 20].

Data were collected from 45 patients (age range 31-78). According to the Breast Imaging and Reporting Data System (BI-RADS) mammographic density categories, reported in Table 2, breast types were classified by an expert radiologist.

Table 2: BI-RADS mammographic density categories and their description.

BI-RADS	Description
1	almost entirely fat
2	scattered fibroglandular densities
3	heterogeneously dense
4	extremely dense

For each patient, optical images in cranio-caudal and oblique views were recorded for both breasts. Tissue composition and scattering parameters were estimated from time-resolved transmittance data by using a global spectral fit procedure [45] and averaged over each image in order to investigate their dependence on mammographic density.

As shown in Figure 10, several parameters obtained from optical data proved to correlate with mammographic breast density: water, lipid and collagen content, as well as the scattering power *b* [19].

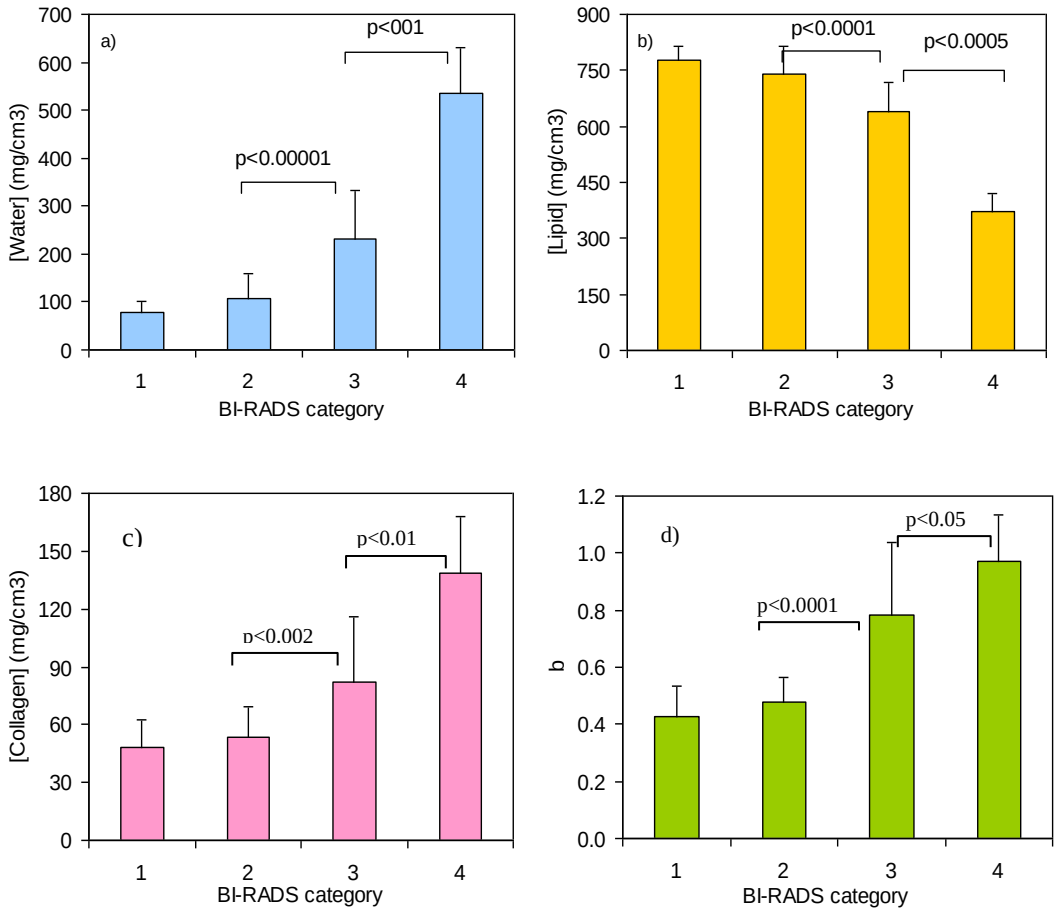

Figure 10: Water (a), lipid (b), collagen (c) concentration and scattering power *b* (d) versus BI-RADS categories. Results are expressed as mean ± SD and refer to the intersubject variability. Mann-Whitney test was used to estimate statistical significance of the difference between the different categories.

Water content increases progressively and significantly with breast density. Correspondingly, a gradual decrease is observed in lipid content. The amount of collagen also increases for increasing breast density. For all the three main constituents, the difference between categories is always highly significant (Mann-Whitney test), except in some cases between category 1 and 2. Since the scattering power *b* provides information on the microscopic tissue structure that is at the origin of breast density, also this parameter was considered and a progressive increase is observed for increasing density.

Since their contributions may not be fully independent, their combination could result in improved correlation with mammographic density. All that parameters that showed significant dependence on mammographic breast density were combined in a single optical index *OI*, defined as followed:

$$OI = \frac{[Water][Collagen]b}{[Lipid]} \quad (5.1)$$

where parameters that are expected to increase with breast density (i.e., the concentrations of water and collagen, and the scattering slope *b*) are all multiplied, and divided by lipid concentration, which conversely is expected to decrease upon increasing breast density. A good correlation was achieved between breast density estimated using conventional mammography and the optical index, as reported in Figure 11.

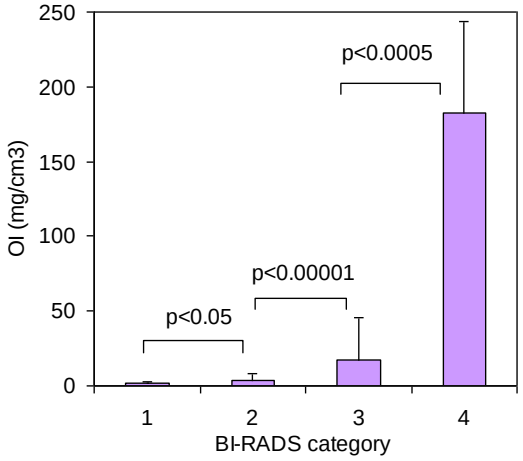

Figure 11: OI versus BI-RADS categories. Results are expressed as mean ± SD and refer to the intersubject variability. Mann-Whitney test was used to estimate statistical significance of the difference between the different categories.

In particular, Figure 11 shows that the optical index can significantly separate category 4 (highest cancer risk) from category 3, with a very good significance ($p < 0.0001$) and category 4 from all the others with even higher confidence.
For the first time, the direct correlation between mammographic density and tissue composition, in terms of the main constituents estimated from optical data, was performed. The clinical study is still in progress, so data from a wider population are becoming available for deeper investigations. Moreover, more sophisticated statistical methods have been used for the correlation between optical and radiological data, showing very promising results for the identification of subjects at high risk to develop breast cancer [46].

6. CONCLUSIONS AND FUTURE PERSPECTIVES

In vivo time-resolved diffuse optical imaging and spectroscopy of breast tissue has been widely investigated in the last few decades. Technological advances in both pulsed light sources, fast detector and time-resolved acquisition electronics allowed the fabrication of compact and accurate devices suitable for the clinical environment.
From what concerns light injection, the time domain approach can benefit from pulsed laser sources with tens of picosecond duration, tens of MHz repetition rate, and average power in the order of few mW. On the detection side, it can benefit from state-of-the-art TCSPC electronics with picosecond resolution and acquisition frequency in the order of few MHz. Moreover, this approach has the advantage to uncouple absorption from scattering contributions, leading to reconstruct the constituent concentrations of the investigated tissue and thus providing a wide range of information useful for diagnostic purposes and for the study of physiological processes.
Different research directions of the time-resolved technique were considered, such as lesion detection by time-gated analysis [22,27], tumour detection with contrast agents [33], monitoring of neoadjuvant chemotherapy [39], and assessment of cancer risk [19].
Most of the presented imaging studies were based on the use of laser sources in the spectral range below 800 nm, where absorption of blood is dominant. In fact, currently the detection of lesions is essentially based on the quantification of haemoglobin since tumours are characterized by an increased vascularisation with respect to the healthy tissue. It is also emerging that an increase of the connective component (water and collagen related) could be associated to the presence of a tumour. Furthermore, for a correct quantification of the breast tissue composition, it is important that all chromophores which contribute to the absorption of the breast tissue are considered. Therefore, the extension of the spectral range to the near infrared region for the quantification also

of lipid, water and collagen is necessary. The Milan group is the only one operating in the time domain that focused the attention on the wide spectral range and extended it over the years up to covering the whole therapeutic window.
Even though for most of the presented research directions the technique needs to be validated on a wider population, as outlined in this chapter, time-resolved optical imaging techniques using near infrared light may have the potential to assist the identification and characterization of breast lesions as well as monitor the response to therapy and estimate cancer risk.
In the future, the spectral range extension could be one of the fundamental keys for the investigation of lesion components to distinguish them between benign and malignant, thus providing a specific diagnostic tool. This aspect of course involves the use of several or tunable laser sources. Moreover, appropriate efficient detectors need to be identified to effectively cover the spectral range of interest.

REFERENCES

1. F. Bray, P. McCarron and D. M. Parkin, "The changing global patterns of female breast cancer incidence and mortality, " *Breast Cancer Res*, 2004, **6**, 229–39.
2. http://www.cancer.gov/
3. L. Tabar, M.-F. Yen, B. Vitak, H.-H. T. Chen, R. A. Smith and S. W. Duffy, "Mammography service screening and mortality in breast cancer patients: 20-year follow-up before and after introduction of screening, " *Lancet*, 2003, **361**, 1405–1410.
4. E. Marshall, Brawling over Mammography, *Science*, 2010, **327**, 936-938.
5. T.M. Kolb, J. Lichy and J.H. Newhouse, "Comparison of the performance of screening mammography, physical examination and breast US and evaluation of factors that influence them: An analysis of 27, 825 patient evaluations, " *Radiology*, 2002, **225**, 165-175.
6. C. K. Kuhl, S. Schrading, C. C. Leutner, N. Morakkabati-Spitz, E. Wardelmann, R. Fimmers, W. Kuhn, and H. H. Schild, "Mammography, breast ultrasound, and magnetic resonance imaging for surveillance of women at high familial risk for breast cancer," J. Clin. Oncol., 2005, **23,** 8469-8476.
7. M. Nothacker, V. Duda, M. Hahn, M. Warm, F. Degenhardt, H. Madjar, S. Weinbrenner and U.-S. Albert, "Early detection of breast cancer: benefits and risks of supplemental breast ultrasound in asymptomatic women with mammographically dense breast tissue. A systematic review, " *BMC Cancer*, 2009, **9**, 335.
8. W.A. Berg, Rationale for a Trial of Screening Breast Ultrasound: American College of Radiology Imaging Network (ACRIN), *AJR*, 2003, 180
9. D. Wu and S.S. Gambhir, "Positron emission tomography in diagnosis and management of invasive breast cancer: Current status and future perspectives, " *Clinical Breast Cancer*, 2003, **4**, S55-S63.
10. F.S. Azar, K. Lee, A. Khamene, R. Choe, A. Corlu, S.D. Konecky, F. Sauer and A.G. Yodh, "Standardized platform for coregistration of nonconcurrent diffuse optical and magnetic resonance breast images obtained in different geometries, " *J. Biomed. Opt.*, 2007, **12**. 051902.
11. S. Srinivasan, C.M. Carpenter, H.R. Ghadyani, S.J. Taka, P.A. Kaufman, R.M. Diflorio-Alexander, W.A. Wells, B.W. Pogue and K.D. Paulsen, "Image guided near-infrared spectroscopy of breast tissue in vivo using boundary element method, " *J. Biomed. Opt.*, 2010, **15**, 061703.
12. Q. Fang, J. Selb, S.A. Carp, G. Boverman, E.L. Miller, D.H. Brooks, R.H. Moore, D.B. Kopans and D.A. Boas, "Combined optical and X-ray tomosynthesis breast imaging," *Radiology*, 2011, **258**, 89-97.
13. Q. Zhu, P.U. Hedge, A. Ricci, M. Kane, E.B. Cronin, Y. Ardeshirpour, C. Xu, A. Aguirre, S.H. Kurtzman, P.J. Deckers and S. Tannenbaum, "Early-stage invasive breast cancers:

Potential role of optical tomography with US localization in assisting diagnosis, " *Radiology*, 2010, **256**, 367-378.
14. F. Martelli, S. Del Bianco, A. Pifferi, L. Spinelli, A. Torricelli and G. Zaccanti, "Hybrid heuristic time dependent solution of the radiative transfer equation for the slab," *Proc. SPIE*, 2009, **7369**, 73691C.
15. J.B. Fishkin and E. Gratton, "Propagation of photon-density waves in strongly scattering media containing an absorbing semi-infinite plane bounded by a straight edge, " *J. Opt. Soc. Am. A*, 1993, **10**, 127-140.
16. F. Martelli, *Light Propagation through Biological Tissue and other Diffusive Media (*2010)
17. M. Cutler, "Transillumination of the breast, " *Surg. Gynecol. Obstet.*, 1929, **48**, 721-727.
18. W. Becker, "Advanced Time-Correlated Single Photon Counting Techniques, " Springer, 2005.
19. P. Taroni, A. Pifferi, G. Quarto, L. Spinelli, A. Torricelli, F. Abbate, A. Villa, N. Balestreri, S. Menna, E. Cassano and R. Cubeddu, Non-invasive assessment of breast cancer risk using time-resolved diffuse optical spectroscopy, *J. Biomed. Opt.*, 2010,**15**, 060501.
20. P. Taroni, A. Pifferi, E. Salvagnini, L. Spinelli, A. Torricelli, and R. Cubeddu, "Seven-wavelength time-resolved optical mammography extending beyond 1000 nm for breast collagen quantification," Opt. Express , 2009, **17,** 15932-15946.
21. D. Grosenick, K. T. Moesta, M. Möller, J. Mucke, H. Wabnitz, B. Gebauer, C. Stroszczynski, B. Wassermann, P. M. Schlag and H. Rinneberg, Time-domain scanning optical mammography: I. Recording and assessment of mammograms of 154 patients, *Phys. Med. Biol.*, 2005, **50**, 2429–2449.
22. P. Taroni, A. Torricelli, L. Spinelli, A. Pifferi, F. Arpaia G. Danesini and R. Cubeddu, Time-resolved optical mammography between 637 and 985 nm: Clinical study on the detection and identification of breast lesions, *Phys. Med. Biol.*, 2005, **50**, 2469-2488.
23. M. S. Patterson, B. Chance and B. C. Wilson , "Time-resolved reflectance and transmittance for the noninvasive measurement of tissue optical properties," *Appl. Opt.*, 1989, **28** 2331–6
24. R. C. Haskell, L. O. Svasaand, T. T. Tsay, T. C. Feng, M. S. McAdams and B. J. Tromberg "Boundary conditions for the diffusion equation in radiative transfer, " *J. Opt. Soc. Am.*, 1994, A **11** 2727–41
25. P. Taroni, A. Pifferi, A. Torricelli, L. Spinelli, G. M. Danesini and R. Cubeddu, "Do shorter wavelengths improve contrast in optical mammography?, " *Phys. Med. Biol.*, 2004b, **49** 1203–15
26. A. Pifferi, A. Torricelli, P. Taroni, D. Comelli and R. Cubeddu, "Optical characterization of primary tissue components by time-resolved reflectance and transmittance spectroscopy, " *Int. Symp. on Biomedical Optics*, 2001, (San Jose, CA, 20–26 Jan.)
27. D. Grosenick, H. Wabnitz, K.T. Moesta, J. Mucke, P.M. Schlag and H. Rinneberg, Time-domain scanning optical mammography: II. Optical properties and tissue parameters of 87 carcinomas, *Phys. Med. Biol.*, 2005, **50**, 2451–2468.
28. L. Spinelli, A. Torricelli, A. Pifferi, P. Taroni, G. Danesini and R.Cubeddu, Characterisation of female breast lesions from multi-wavelength time-resolved optical mammography, *Phys. Med. Biol.*, 2005, **50**, 2489–2502.
29. T. Yates, J. C. Hebden, A. Gibson, N. Everdell, S. R. Arridge and M. Douek, "Optical tomography of the breast using a multi-channel time-resolved imager, "Phys. Med. Biol., 2005, **50** 2503–2517.
30. X. Intes, "Time-domain optical mammography SoftScan: initial results," Acad. Radiol., 2005, **12,** 934-947.
31. Y. Ueda, K. Yoshimoto, E. Ohmae, T. Suzuki, T. Yamanaka, D. Yamashita, H. Ogura, C. Teruya, H. Nasu, E. Ima, H. Sakahara, M. Oda, Y. Yamashita, "Time-resolved optical mammography and its preliminary clinical results, " Technol Cancer Res Treat., 2011, **10**, 393-401.

32. A. Hagen , D. Grosenick, R. Macdonald, H. Rinneberg, S. Burock, P. Warnick, A. Poellinger, and P. M. Schlag, "Late-fluorescence mammography assesses tumor capillary permeability and differentiates malignant from benign lesions, " *Opt Express* 2009 , **17** ,17016 – 17033 .
33. D. Grosenick, A. Hagen, O. Steinkellner, A. Poellinger, S. Burock, P. M. Schlag, H. Rinneberg and R. Macdonald, "A multichannel time-domain scanning fluorescence mammograph: Performance assessment and first in vivo results, " *Scientific Instruments* , 2011, **82**, 024302.
34. A. Poellinger, S. Burock, D. Grosenick, A. Hagen, L. Lüdemann, F. Diekmann, F. Engelken, R. Macdonald, H. Rinneberg and P.-M. Schlag, "Breast cancer: Early- and late-fluorescence near-infrared imaging with indocyanine green, - A preliminary study, " *Radiology*, 2011, **258**, 409-416.
35. D. R. Busch, R. Choe, M. A. Rosen, W. Guo, T. Durduran,.M. D. Feldman, C. Mies, B. J. Czerniecki, J. Tchou, A. De Michele, M. D. Schnall, and A. G. Yodh, "Optical malignancy parameters for monitoring progression of breast cancer neoadjuvant chemotherapy, " *Biomedical Optics Express*, 2012, **4**, 105-121.
36. D. B. Jakubowski, A. E. Cerussi, F. Bevilacqua, N. Shah, D. Hsiang, J. Butler, and B. J. Tromberg, "Monitoring neoadjuvant chemotherapy in breast cancer using quantitative diffuse optical spectroscopy: a case study," *J. Biomed. Opt.* , 2004, **9,** 230-238.
37. L. C. Enfield, A. P. Gibson, N. L. Everdell, D. T. Delpy, M. Schweiger, S. R. Arridge, C. Richardson, M. Keshtgar, M. Douek, and J. C. Hebden, "Three-dimensional time-resolved optical mammography of the uncompressed breast, " *Ap. Opt*., 2007, **46**, 3628-3638.
38. S. R. Arridge, J. C. Hebden, M. Schweiger, F. E. W. Schmidt, M. E. Fry, E. M. C. Hillman, H. Dehghani, and D. T. Delpy, "A method for 3D time-resolved optical tomography," *Int. J. Imaging Syst. Technol.*, 2000, **11,** 2–11.
39. L. Enfield, G. Cantanhede, M. Douek, V. Ramalingam, A. Purushotham, J. Hebden, and A. Gibsona, "Monitoring the response to neoadjuvant hormone therapy for locally advanced breast cancer using three-dimensional time-resolved optical mammography, " *Journal of Biomedical Optics*, 2013, **18**, 056012(1-6).
40. V. A. McCormack and I. dos Santos Silva, "Breast Density and Parenchymal Patterns as Markers of Breast Cancer Risk: A Meta-analysis," *Cancer Epidemiol. Biomarkers Prev.* **15**, 1159-1169 (2006).
41. N. F. Boyd, H. Guo, L. J. Martin, L. Sun, J. Stone, E. Fishell, R. A. Jong, G. Hislop, A. Chiarelli, S. Minkin, and M. J. Yaffe, "Mammographic Density and the Risk and Detection of Breast Cancer," *N. Engl. J. Med.* **356**, 227-236 (2007).
42. C. Byrne, "Studying mammographic density: implications for understanding breast cancer," *J. Natl. Cancer Inst*. **89,** 531-533 (1997).
43. V. A. McCormack and I. dos Santos Silva, "Breast density and parenchymal patterns as markers of breast cancer risk: a meta-analysis," *Cancer Epidemiol. Biomarkers Prev*. **15,** 1159-1169 (2006).
44. P. Taroni, D. Comelli, A. Pifferi, A. Torricelli, and R. Cubeddu, "Absorption of collagen: effects on the estimate of breast composition and related diagnostic implications," *J. Biomed. Opt*. **12,** 014021 (2007).
45. C. D'Andrea, L. Spinelli, A. Bassi, A. Giusto, D. Contini, J. Swartling, A. Torricelli, and R. Cubeddu, "Time-resolved spectrally constrained method for the quantification of chromophore concentrations and scattering parameters in diffusing media," *Opt. Express*, 2006**, 14,** 1888-1898.
46. P. Taroni, G. Quarto, A. Pifferi, F. Ieva, A. M. Paganoni, F. Abbate, N. Balestreri, S. Menna, E. Cassano, and R. Cubeddu, " Optical Identification of Subjects at High Risk for Developing Breast Cancer,"*J. Biomed. Opt*., 2013, **18**, 060507-3.

47. P. Taroni, A. Torricelli, L. Spinelli, A. Pifferi, F. Arpaia G. Danesini and R. Cubeddu, Time-resolved optical mammography between 637 and 985 nm: Clinical study on the detection and identification of breast lesions, Phys. Med. Biol., 2005, **50**, 2469-2488.